



Diinosine pentaphosphate (IP₅I) is a potent antagonist at recombinant rat P2X₁ receptors

*¹B.F. King, ¹M. Liu, ²J. Pintor, ²J. Gualix, ²M.T. Miras-Portugal & ¹G. Burnstock

¹Autonomic Neuroscience Institute, Royal Free & University College Medical School, Royal Free Campus, Rowland Hill Street, Hampstead, London NW3 2PF and ²Departamento de Bioquímica, Facultad de Veterinaria, Universidad Complutense, 28040 Madrid, Spain

1 The antagonist activity of a series of diinosine polyphosphates (Ip_nI, where $n=3, 4, 5$) was assessed against ATP-activated inward currents at rat P2X_{1–4} receptors expressed in *Xenopus* oocytes and studied under voltage-clamp conditions.

2 Diinosine polyphosphates were prepared by the enzymatic degradation of their corresponding diadenosine polyphosphates (e.g., Ap₅A into Ip₅I) using 5'-adenylic deaminase, and purified using reverse-phase chromatography.

3 Against ATP-responses at rP2X₁ receptors, the potency order for antagonism was (pIC₅₀): Ip₅I (8.5)>Ip₄I (6.3)>Ip₃I (>4.5). Ip₅I (10–100 nM) caused a concentration-dependent rightwards displacement of the ATP concentration-response curve without reducing the maximum ATP effect. However, the Schild plot was non-linear which indicated Ip₅I is not a competitive antagonist. Blockade by micromolar concentrations of Ip₅I was not surmountable. Ip₄I also behaved as a non-surmountable antagonist.

4 Against ATP-responses at rP2X₃ receptors, the potency order for antagonism was (pIC₅₀): Ip₄I (6.0)>Ip₅I (5.6)>Ip₃I (>4.5). Blockade by Ip₄I (pA₂, 6.75) and Ip₅I (pA₂, 6.27) was surmountable at micromolar concentrations.

5 Diinosine polyphosphates failed to inhibit ATP-responses at rP2X₂ receptors, whereas agonist responses at rP2X₄ were reversibly potentiated by Ip₄I and Ip₅I. None of the parent diadenosine polyphosphates behave as antagonists at rP2X_{1–4} receptors.

6 Thus, Ip₅I acted as a potent and relatively-selective antagonist at the rP2X₁ receptor. This dinucleotide pentaphosphate represents a high-affinity antagonist for the P2X₁ receptor, at which it acts in a competitive manner at low (≤ 100 nM) concentrations but has more complex actions at higher (> 100 nM) concentrations.

Keywords: P2X receptor; ion channel; ATP; dinucleotide; Ip₅I; diinosine polyphosphate; antagonist; *Xenopus* oocyte

Abbreviations: ATP, adenosine 5'-triphosphate; Ap₅A, diadenosine pentaphosphate; D- β , γ -meATP, D isomer of β , γ -methylene ATP; L- β , γ -meATP, L isomer of β , γ -methylene ATP; DIDS, 4,4'-diisothiocyanostilbene-2,2'-disulphonic acid; I_{ATP}, ATP-activated membrane current; IC₅₀, concentration causing 50% reduction of agonist response; Ip₃I, diinosine triphosphate; Ip₄I, diinosine tetraphosphate; Ip₅I, diinosine pentaphosphate; KN-62, 1-[N,O-bis(5-isoquinolinesulphonyl)-N-methyl-L-tyrosyl]-4-phenylpiperazine; MRS 2220, cyclic pyroxidine- α ^{4,5}-monophosphate-6-azophenyl-2',5'-disulphonic acid; NF023, 8,8'-(carbonylbis(imino-3,1-phenylene carbonyliminobis-(1,3,5-naphthalenetrisulphonic acid)); n_H, Hill coefficient; pA₂, negative log of antagonist concentration causing a 2 fold decrease in agonist potency; pEC₅₀, negative log of agonist concentration causing 50% reduction of agonist response; pIC₅₀, negative log of antagonist concentration causing 50% reduction of agonist response; PPADS, pyridoxal- α ⁵-phosphate-6-azophenyl-2',4'-disulphonic acid; rP2X_{1–4}, rat P2X_{1–4} receptor subtypes, RB-2, Reactive blue 2; TNP-ATP, 2',3'-O-(2,4,6-trinitrophenol)-ATP; V_h, holding potential

Introduction

P2X receptors are ATP-gated cation channels composed of oligomeric assemblies of three, or possibly four, receptor protein subunits (Kim *et al.*, 1997; Nicke *et al.*, 1998; Torres *et al.*, 1999). Seven P2X subunits (P2X_{1–7}) have been cloned thus far, the operational profiles and pharmacological characteristics of homomeric assemblies of P2X_{1–7} receptors having been well documented (for reviews, see: Evans *et al.*, 1998; Humphrey *et al.*, 1998; King, 1998). Transcripts for P2X_{1–4} receptor proteins are abundant in excitable tissues (neurons, smooth muscle, cardiac muscle) and in secretory epithelia, while the distribution of P2X₅ and P2X₇ mRNA is highly restricted. P2X₆ transcripts are especially abundant in the neuraxis (Collo *et al.*, 1996), but it remains controversial that

the P2X₆ subunit protein is capable of forming homomeric assemblies (Torres *et al.*, 1999).

The correspondence between homomeric P2X receptors and native P2X receptors has been hampered by a paucity of selective ligands for P2X subunits. Operational profiles of homomeric P2X receptors have been matched loosely to some examples of native P2X receptors (Evans & Surprenant, 1996), but the possibility of subpopulations of homomeric and heteromeric P2X receptors in any pool of native P2X receptors cannot be discounted. Some progress has been made with agonists showing reasonable P2X subunit selectivity, e.g. L- β , γ -meATP at P2X₁ receptors (Evans *et al.*, 1995), D- β , γ -meATP at P2X₃ receptors (Rae *et al.*, 1998), and activity series of the diadenosine polyphosphates (Ap_nA, where $n=2–6$) at P2X_{1–4} receptors (Wildman *et al.*, 1999a). However, differentiating homomeric P2X receptors by agonist activity alone is a lengthy and laborious process (Humphrey *et al.*, 1998). Further

*Author for correspondence; E-mail: b.king@ucl.ac.uk

progress has been made with P2X subunit-selective antagonists: the anion transport inhibitor, DIDS, is relatively selective for P2X₁ receptors at micromolar concentrations (Evans *et al.*, 1995); the PPADS derivative, MRS 2220, is wholly selective for P2X₁ receptors at micromolar concentrations (Jacobson *et al.*, 1998); the suramin analogue, NF023, is a potent antagonist at P2X₁ receptors at submicromolar concentrations, whilst 35–138 fold less potent at species orthologues of P2X₃ receptors (Soto *et al.*, 1999); TNP-ATP is a potent antagonist at both P2X₁ and P2X₃ receptors at nanomolar concentrations (Virginio *et al.*, 1998); KN-62 is a potent antagonist of P2X₇ receptors, although it shows differential activity at species orthologues of the P2X₇ receptor (Humphreys *et al.*, 1998). Neither suramin, PPADS nor Reactive blue 2 (RB-2) readily discriminate between P2X subunits (Evans *et al.*, 1998; King, 1998; Ralevic & Burnstock, 1998).

Diinosine polyphosphates (abbreviated Ip_nI, where *n* is the number of phosphates) comprise two ribosylated inosine molecules bridged by a phosphate chain. These dinucleotides are synthesized by deaminating diadenosine polyphosphates with the non-specific AMP-deaminase of *Aspergillus sp.* (Guranowski *et al.*, 1995; Pintor *et al.*, 1997). One member of this family, P¹,P⁵-bis(5'-inosyl) pentaphosphate (Ip₅I), has already shown interesting pharmacological properties, being a potent antagonist at: (i) a specific dinucleotide receptor for diadenosine polyphosphates in rat brain synaptosomes (IC₅₀ value, 4 nM); (ii) a P2X receptor in the same preparation (IC₅₀ value, 30 μ M); (iii) the P2X₁-like receptor in guinea-pig isolated vas deferens (pA₂ value, 6.5) (Hoyle *et al.*, 1997; Pintor *et al.*, 1997; 1999). In this paper, we describe the antagonist properties of Ip₅I and two related dinucleotides, Ip₄I and Ip₃I, on homomeric P2X_{1–4} receptors. The activity profile of dinucleotide pentaphosphate reveals selectivity for the P2X₁ receptor subtype at nanomolar concentrations.

Methods

Diinosine polyphosphate synthesis

Diinosine pentaphosphate (Ip₅I) was prepared by enzymatic degradation of diadenosine pentaphosphate (Ap₅A). Ip₄I and Ip₃I were also prepared in the same manner from Ap₄A and Ap₃A, respectively. 5'-adenylic acid deaminase (0.12 U) from *Aspergillus sp.* was incubated with 10 mM Ap₅A in a final volume of 1 ml of 50 mM HEPES (pH 6.5) for 90 min (at 37°C). Aliquots (10 μ l) were taken at different times, placed in 100°C water bath for 5 min to stop the enzymatic reaction, and diluted 1:100 with distilled water to monitor the production of Ip₅I by HPLC techniques. After 90 min, the reaction was stopped by boiling the incubation medium at 100°C for 5 min, after which protein debris was removed by filtration through a Millex-G5 filter (0.22 μ m; from Millipore). The reaction product was confirmed as Ip₅I by HPLC detection. Samples were treated with phosphodiesterase (3 mU, at 37°C) from *Crotalus durissus* (EC.3.1.15.1) (for rationale, see Results) then diluted 1:100 with distilled water for HPLC separation and detection of Ip₅I breakdown products.

Chromatographic procedures

The chromatographic equipment consisted of a Waters 600E delivery system, a Waters 717+ autosampler and a Waters 2487 dual wavelength absorbance detector, which were managed by Millenium 2010 software. Analyses were performed under reverse-phase chromatography conditions,

equilibrating the system with 100 mM KH₂PO₄, 4% methanol, pH 6.0, at 1.5 ml min⁻¹. The column was a Spherisorb ODS-2 (25 cm length, 0.4 cm diameter; from Waters). Detection was monitored at 260 nm wavelength. For phosphodiesterase measurements, ion-pair chromatography was performed. The mobile phase conditions were 10 mM KH₂PO₄, 2 mM tetrabutyl ammonium, 15% acetonitrile, pH 7.5, at 2 ml min⁻¹. The column was a Spherisorb ODS-2. Detection was performed as above.

Oocyte preparation

Xenopus laevis frogs were anaesthetized in Tricaine (0.2% w v⁻¹), killed by decapitation, and the ovarian lobes removed surgically. Oocytes (stages V and VI) were defolliculated by a 2-step process involving collagenase treatment (Type IA, 2 mg ml⁻¹ in a Ca²⁺-free Ringer's solution, for 2–3 h) followed by stripping away the follicular layer with fine forceps. Defolliculated oocytes were stored in Barth's solution (pH 7.5, at 4°C) containing (mM): NaCl, 110; KCl, 1; NaHCO₃, 2.4; Tris HCl, 7.5; Ca(NO₃)₂, 0.33; CaCl₂, 0.41; MgSO₄, 0.82; gentamycin sulphate, 50 μ g l⁻¹. Separate batches of defolliculated oocytes were injected cytosolically (40 nl, 1 μ g ml⁻¹) with cRNAs for rat P2X_{1–4} receptors (see Acknowledgements), incubated for 24–48 h at 18°C in Barth's solution and, thereafter, kept at 4°C for up to 12 days until used in electrophysiological experiments.

Electrophysiology

ATP-evoked membrane currents (I_{ATP}) (V_h = -60 to -90 mV) were recorded from cRNA-injected oocytes using a twin-electrode voltage-clamp amplifier (Axoclamp 2B). The voltage-recording and current-recording microelectrodes (1–5 M Ω tip resistance) were filled with 3.0 M KCl. Oocytes were superfused with a Ringer's solution (5 ml min⁻¹, at 18°C) containing (mM): NaCl, 110; KCl, 2.5; HEPES, 5; BaCl₂, 1.8, adjusted to pH 7.5. The extracellular pH was maintained at pH 7.5 in all experiments, since the potency of ATP at P2X_{1–4} receptors is affected by H⁺ ions (King *et al.*, 1996; Wildman *et al.*, 1999b,c).

Solutions and drugs

All solutions were nominally Ca²⁺-free to avoid the activation of a Ca²⁺-dependent Cl⁻ current ($I_{Cl, Ca}$) in oocytes. ATP was prepared in Ca²⁺-free Ringer's solution at the concentrations stated, and superfused *via* a gravity-feed continuous flow system which allowed rapid addition and washout. Ip_nI compounds were dissolved in a buffer solution (HEPES 50 mM, pH 6.5 with KOH) to give a 10 mM stock solution, then diluted further using Ringer's solution and readjusted to pH 7.5. For inhibition curves, ATP (at the EC₇₀ value at pH 7.5 (in μ M): P2X₁, 1; P2X₂, 20; P2X₃, 3; P2X₄, 10) was added to the superfusate for 60–120 s, then washed off with Ringer's solution for 30 min. After obtaining agonist responses of consistent amplitude (Figure 1A), diinosine polyphosphates (Ip_nI, 0.1–100,000 nM) were added to the superfusate for 30 min before and during re-application of ATP. The blocking activity of Ip_nI compounds did not improve with pre-incubation periods longer than 10 min (Figure 1B) which suggested that Ip_nI blockade was not use-dependent, although Ip_nI compounds were routinely applied throughout the full 30 min of the ATP-washout period. For Schild analyses, the concentration/response (C/R) relationship was determined for ATP (0.01–300 μ M), then cRNA-injected oocytes were

incubated with Ip_nI compounds for 30 min, after which ATP C/R curves constructed again in the continued presence of Ip_nI . EC₅₀ values and slopes of C/R curves were taken from Hill plots, using the transform $\log (I/I_{max}-I)$ where I is the current evoked by each concentration of ATP. pA₂ values were determined by Schild analysis, using the equation $\{\log (DR-1)-\log [Ip_nI]\}$.

Statistics

Data are presented as means \pm s.e.mean of 4–6 sets of data from different oocyte batches. Significant differences were determined by either unpaired or paired Student's *t*-test using commercially-available software (InStat v2.05a, GraphPad).

Materials

All common salts were AnalaR grade (Aldrich Chemicals, U.K.). Adenosine 5'-triphosphate, diadenosine polyphosphates (Ap₃A, Ap₄A, Ap₅A) and phosphodiesterase (EC.3.1.15.1) (from *Crotalus durissus*) were purchased from Boehringer (Mannheim, Germany). 5'-adenylic acid deaminase

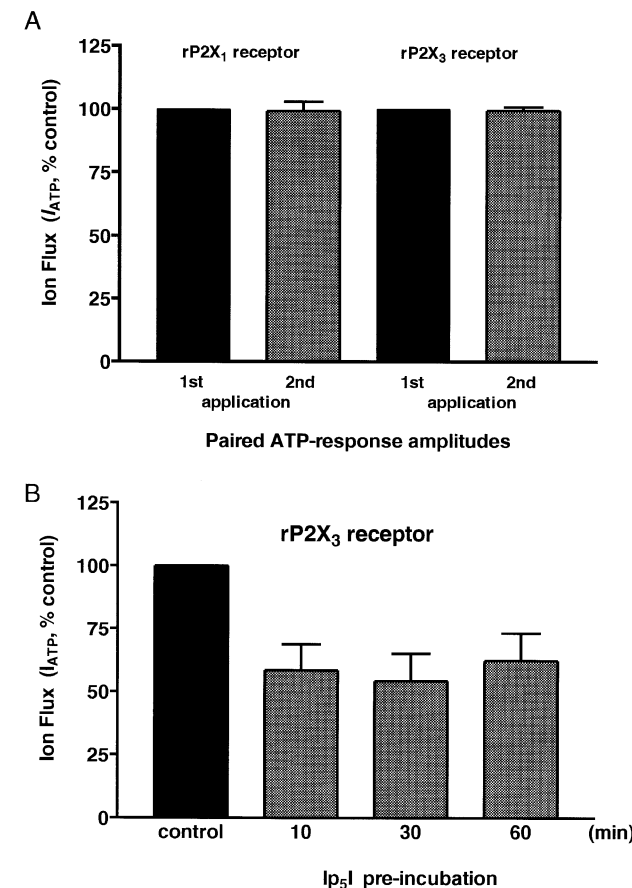


Figure 1 Consistency of agonist and antagonist activity. (A) histograms of the amplitudes of paired agonist-responses at homomeric rP2X₁ and rP2X₃ receptors (using ATP: rP2X₁, 1 μ M; rP2X₃, 3 μ M). Washout periods of 30 min were used between first and second applications of ATP, a periodicity sufficient to yield I_{ATP} responses of consistent amplitude. Thus, Ip_nI -related antagonism could not be explained in terms of a rundown of ATP-responses at P2X₁ and P2X₃ receptors. (B) the effect of increasing the pre-incubation period (10, 30 and 60 min) to Ip₅I (3 μ M) on the level of antagonism of ATP-responses (using 3 μ M) at homomeric rP2X₃ receptors. The blocking activity of Ip₅I neither improved nor waned over 60 min pre-incubation, indicating that blockade was not use-dependent. Data: mean \pm s.e.mean ($n=4$) in A and B.

(from *Aspergillus sp.*) was purchased from Sigma Chemical Co. (St. Louis, U.S.A.).

Results

Production of Ip_nI

5'-adenylic acid deaminase of *Aspergillus sp.* efficiently transformed Ap₅A into Ip₅I, fully converting the substrate into product over 90 min without further transformation of Ip₅I into other by-products. During intermediate times, HPLC analysis of the reaction medium revealed an additional peak with a retention time between that of the initial Ap₅A peak and final Ip₅I peak (Figure 2A). This additional peak gradually disappeared over 90 min and was attributed to the intermediary reaction product (Ip₅A), where only one of two adenosine moieties had been deaminated. Like results were obtained when producing Ip₄I from Ap₄A and Ip₃I from Ap₃A.

The final reaction product was confirmed as Ip₅I (as opposed to related breakdown products, i.e. IMP and Ip₄) in experiments where phosphodiesterase was used. This enzyme cleaves Ip₅I to yield inosine monophosphate (IMP) and the mononucleotide inosine 5'-tetraphosphate (Ip₄) (Figure 2B). The retention times for these breakdown products was compared and matched against times for standard solutions of IMP and Ip₄. The absence of IMP and Ip₄ peaks (prior to enzymatic treatment at zero time) in HPLC analysis indicated

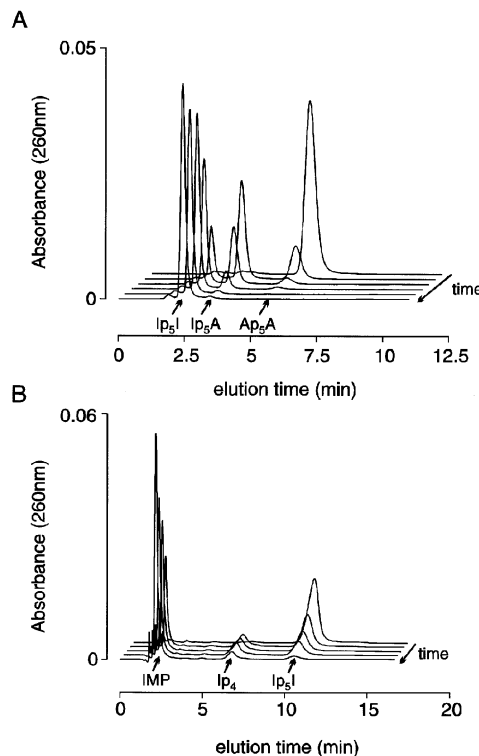


Figure 2 HPLC analysis of Ip₅I production. (A) a series of chromatographic profiles for the time-dependent enzymatic conversion of Ap₅A into the intermediary product Ip₅A and final product Ip₅I by adenylate deaminase (*Aspergillus sp.*) over a period of 90 min (chromatograms at: T = 0, 15', 30, 45', 60' and 90'). (B) a series of chromatographic profiles for the time-dependent production of IMP and Ip₄ by phosphodiesterase breakdown of the reaction product Ip₅I (chromatograms at: T = 0, 5', 10', 15' and 30'). Ordinate scalars (A and B) as AUFS (absorbance units full scale), as defined by Millennium 2010 software (Waters).

Ip₅I had not been broken down during its synthesis. Similar results were observed when testing the purity of Ip₄I and Ip₃I.

Blockade of P2X receptors by Ip₅I

The pentaphosphate Ip₅I (1 μ M) was a potent inhibitor of ATP-responses at rP2X₁ receptors, and weak inhibitor of ATP-responses at rP2X₃ receptors (Figure 3A,B and Table 1). However, Ip₅I failed to block rP2X₂ receptors and potentiated ATP-responses at rP2X₄ receptors (Figure 3C,D and Table 1). Thus, Ip₅I is an antagonist at Group 1 P2X receptors (as defined by Humphrey *et al.*, 1998), yet approximately 900 fold more potent at rP2X₁ than rP2X₃ receptors. The inhibitory and facilitatory effects of Ip₅I were reversed on washout. Micromolar levels of Ip₅I had no effect on the holding current of either *Xenopus* oocytes injected with cRNA for rP2X_{1–4} receptors or water-injected (control) oocytes. Thus, Ip₅I inhibition or facilitation was not due to a partial agonistic effect.

Blockade of P2X receptors by Ip_nI series

The blocking activity Ip₄I and Ip₃I was also investigated at Group 1 P2X receptors (Figure 4A,B and Table 1). Ip₄I was 180 fold less potent than Ip₅I as an antagonist of rP2X₁ receptors yet, in contrast, 3 fold more potent than Ip₅I as an

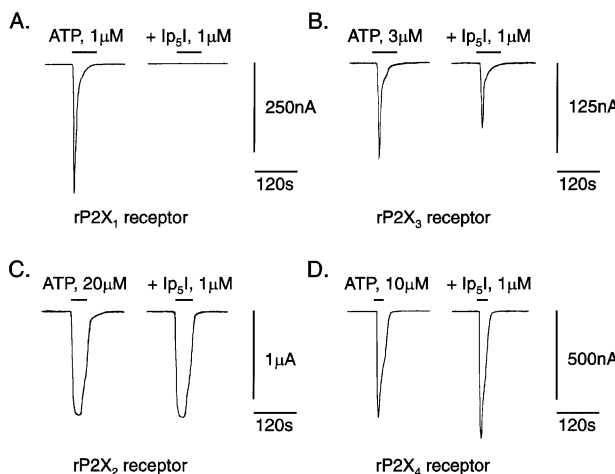


Figure 3 Ip₅I antagonism of ATP-responses at rP2X_{1–4} receptors. ATP-activated whole-cell inward currents (I_{ATP}), before (first record) and during (second record) superfusion of micromolar Ip₅I (1 μ M, 30 min pre-incubation). Paired I_{ATP} records were taken from single cRNA-injected oocytes expressing homomeric rP2X₁ (in A), rP2X₃ (in B), rP2X₂ (in C) and rP2X₄ receptors (in D). ATP was applied at a concentration equivalent to the EC₇₀ value for each recombinant rP2X_{1–4} receptor (see Methods). $V_h = -60$ mV in A–D.

Table 1 Activity indices of Ip_nI compounds at rP2X_{1–4} receptors

Compound	P2X ₁ IC_{50} value	P2X ₂	P2X ₃ IC_{50} value	P2X ₄ EC_{50} value
Ip ₅ I	0.0031 ± 0.0004 μ M (n_H , -0.96 ± 0.08)	inactive (0.1–30 μ M)	2.8 ± 0.7 μ M (n_H , -1.02 ± 0.14)	0.0020 ± 0.0004 μ M (n_H , 1.33 ± 0.09)
Ip ₄ I	0.560 ± 0.080 μ M (n_H , -1.47 ± 0.20)	inactive (0.1–30 μ M)	1.0 ± 0.3 μ M (n_H , -1.16 ± 0.10)	1.69 ± 0.4 μ M (n_H , 2.29 ± 0.17)
Ip ₃ I	> 30 μ M	inactive (0.1–30 μ M)	> 30 μ M	inactive (0.3–10 μ M)

IC₅₀ and EC₅₀ values for the inhibitory and facilitatory effects of Ip_nI compounds on ATP-responses at recombinant P2X_{1–4} receptors. Slopes of inhibition and facilitation curves are given in brackets. Data: mean \pm s.e.mean ($n=5$).

antagonist of P2X₃ receptors. The triphosphate Ip₃I was a weak antagonist of rP2X₁ and rP2X₃ receptors, only showing significant levels of blockade at high concentrations (> 10 μ M). The blocking actions of Ip₄I and Ip₃I were reversed on washout.

The actions Ip₄I and Ip₃I were also studied at rP2X₂ and rP2X₄ receptors (Figure 4A,B and Table 1). Both Ip_nI compounds, like Ip₅I, were inactive as either antagonists or potentiators at rP2X₂ receptors (Figure 5A). At rP2X₄

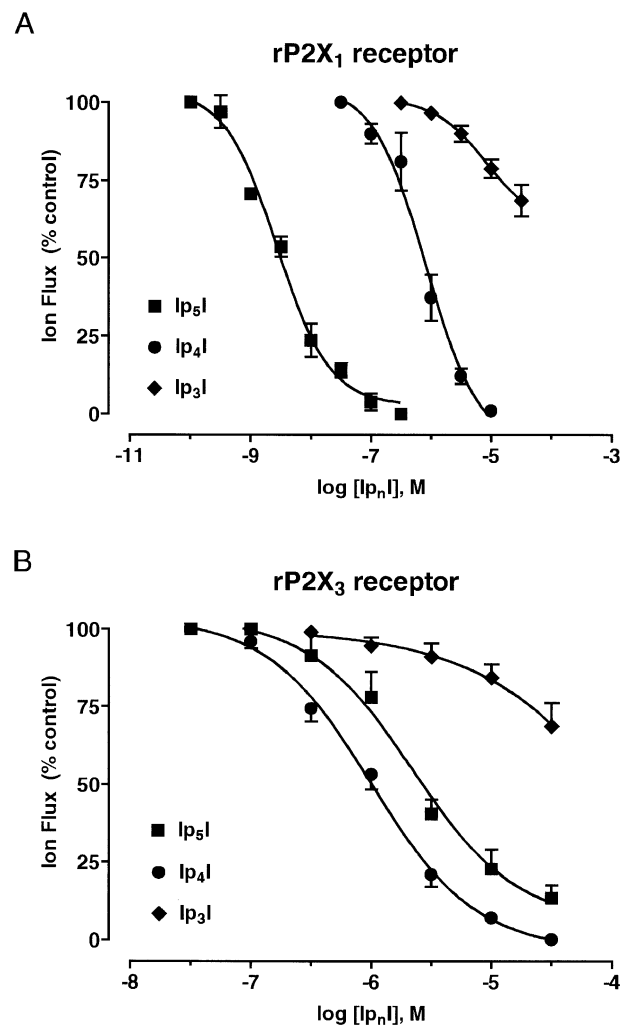


Figure 4 Inhibition curves for Ip_nI series at Group 1 P2X receptors. (A) Concentration-dependent inhibition of I_{ATP} (ATP, 1 μ M) at homomeric rP2X₁ receptors by Ip₅I, Ip₄I and Ip₃I. (B) Concentration-dependent inhibition of I_{ATP} (ATP, 3 μ M) at homomeric rP2X₃ receptors by the same diinosine polyphosphates. IC₅₀ values and slopes of inhibition curves are given in Table 1. Data: mean \pm s.e.mean ($n=5$) in A and B.

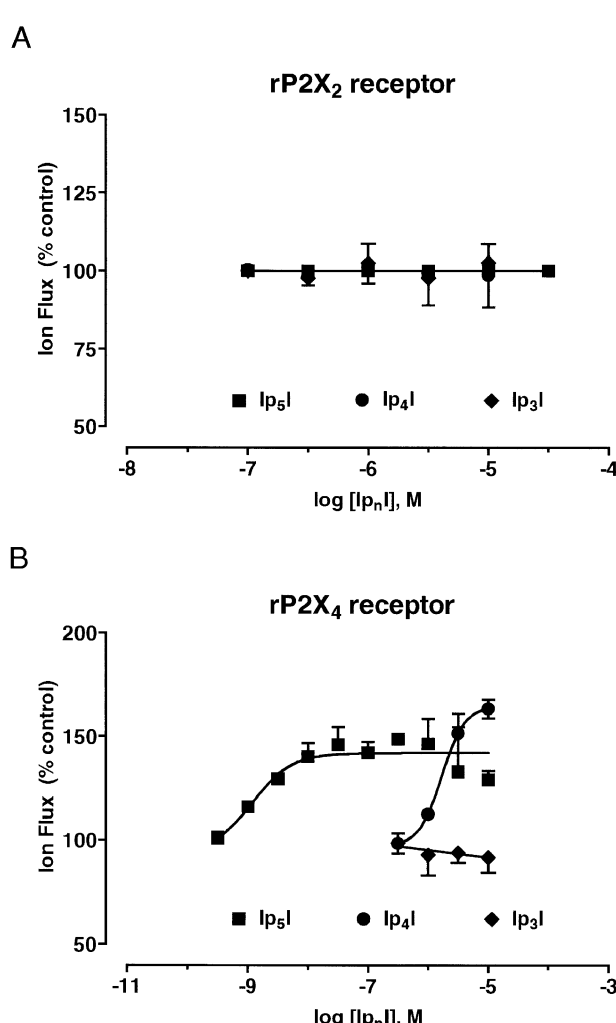


Figure 5 Activity of Ip_nI series at rP2X₂ and rP2X₄ receptors. (A) The Ip_nI series neither inhibited nor potentiated ATP-responses (using 20 μM) at rP2X₂ receptors. (B) Ip_5I and Ip_4I potentiated ATP-responses (using 10 μM) at rP2X₄ receptors. Activity indices for Ip_nI series given in Table 1. Data: mean \pm s.e.mean ($n=5$) in A and B.

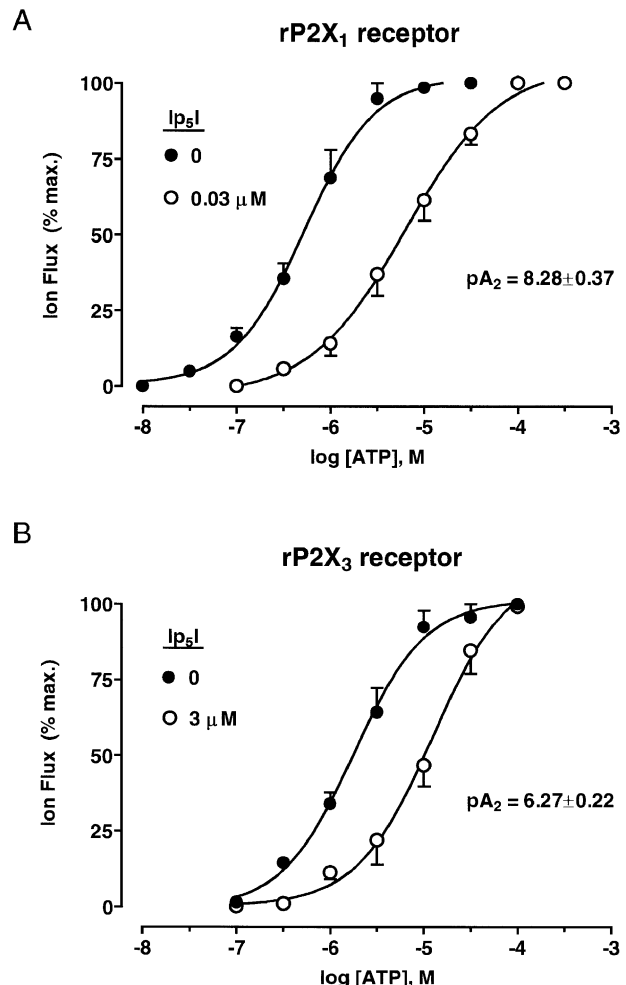


Figure 6 Ip_5I antagonism of ATP-responses at Group 1 P2X receptors. (A) Concentration-response curves for ATP (0.01–300 μM) at homomeric rP2X₁ receptors, before and during the presence of Ip_5I (30 nM). (B) Concentration-response curves for ATP (0.1–100 μM) at homomeric rP2X₃ receptors, before and during the presence of Ip_5I (3 μM). EC₅₀ values, Hill coefficients and pA₂ values given in Table 2. Data: mean \pm s.e.mean ($n=4$) for paired C/R curves, in A and B.

Table 2 Schild analysis of Ip_5I displacement of ATP C/R curves at rP2X₁ receptors

Ip_5I (nM)	EC ₅₀ values and Hill coefficients		pA_2	n
	Control	+ Ip_5I		
10	0.38 \pm 0.07 μM (n_H , 0.96 \pm 0.06)	1.89 \pm 0.87 μM (n_H , 0.89 \pm 0.08)	8.43 \pm 0.29 (range, 7.99–8.89)	4
30	0.42 \pm 0.06 μM (n_H , 0.99 \pm 0.14)	3.56 \pm 2.05 μM (n_H , 0.82 \pm 0.09)	8.28 \pm 0.37 (range, 7.70–8.86)	4
100	0.70 \pm 0.15 μM (n_H , 1.02 \pm 0.15)	92.1 \pm 15.7 μM (n_H , 0.86 \pm 0.16)	8.99 \pm 0.19 (range, 8.49–9.23)	4

EC₅₀ values and Hill coefficients (n_H) for the ATP C/R relationship in the absence (control) and presence (+ Ip_5I) of diinosine pentaphosphate (10–100 nM). Data: mean \pm s.e.mean of paired sets of observations.

receptors, Ip_4I was over 800 fold less potent than Ip_5I at potentiating ATP-responses (an effect reversed on washout), while Ip_3I had no effect (Figure 5B and Table 1).

Schild analysis of Ip_5I blockade

Ip_5I (10, 30 and 100 nM) caused a rightwards displacement of the ATP concentration-response (C/R) curve, without altering the maximum agonist effect (Figures 6A and 8 and Table 2). However, higher concentrations of Ip_5I (1 and 10 μM)

completely blocked the agonist effects of ATP (≤ 1 mM) (Figure 8), beyond which ATP exerts non-specific excitatory effects on *Xenopus* oocytes (Kupitz & Atlas, 1993). Thus, Ip_5I blockade was surmountable at low Ip_5I concentrations (≤ 100 nM), and nonsurmountable at micromolar concentrations. The antagonistic effects of Ip_5I (10–100 nM) on ATP C/R curves (EC₅₀ values, Hill coefficients and pA₂ values) are summarized in Table 2. Schild analysis of paired C/R curves revealed that pA₂ values were not uniform, varying between 7.70–9.23 (range of 12 determinations) for the mean pA₂

values listed (Table 2). This variability, in combination with nonsurmountable blockade with micromolar Ip₅I, indicated that this dinucleotide did not antagonize ATP-mediated membrane currents at rP2X₁ receptors in a simple competitive manner.

On the other hand, high concentrations of Ip₅I (3 μ M, approximate IC₅₀ value) did cause a surmountable antagonism of ATP-responses at rP2X₃ receptors (Figure 6B). EC₅₀ values and Hill coefficients for ATP were (for the following Ip₅I concentrations): 0 μ M, 1.4 \pm 0.4 μ M (n_H, 1.13 \pm 0.12); 3 μ M, 9.6 \pm 2.5 μ M (n_H, 1.08 \pm 0.18) (n=4). The pA₂ value for Ip₅I antagonism at rP2X₃ receptors was 6.27 \pm 0.22 (n=4).

Schild analysis of Ip₄I blockade

Ip₄I (3 μ M, approximate IC₅₀ value) caused a nonsurmountable inhibition of ATP-response at rP2X₁ receptors, in the manner of non-competitive antagonist (Figure 7A). EC₅₀ values and Hill coefficients for ATP were (for the following Ip₄I concentrations) : 0 μ M, 0.38 \pm 0.06 μ M (n_HH, 0.84 \pm 0.17); 3 μ M, 1.91 \pm 0.43 μ M (n_H, 0.63 \pm 0.46) (n=4). The maximum

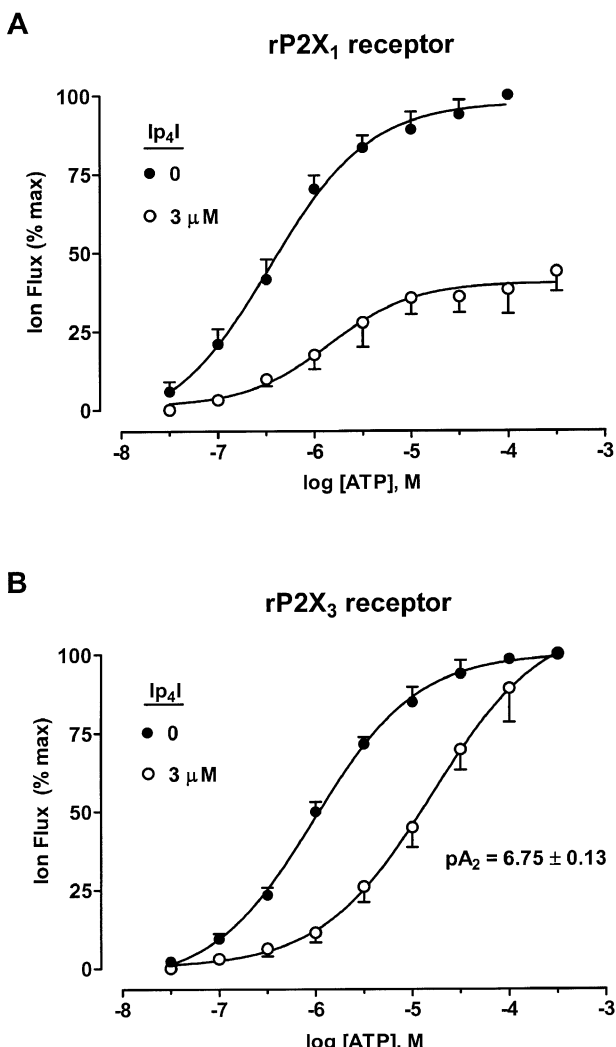


Figure 7 Ip₄I antagonism of ATP-responses at Group 1 P2X receptors. (A) Concentration-response curves for ATP (0.03–300 μ M) at homomeric rP2X₁ receptors, before and during the presence of Ip₄I (3 μ M). (B) Concentration-response curves for ATP (0.03–300 μ M) at homomeric rP2X₃ receptors, before and during the presence of Ip₄I (3 μ M). EC₅₀ values, Hill coefficients and pA₂ values given in the text. Data: means \pm s.e.mean (n=4) for paired C/R curves, in A and B.

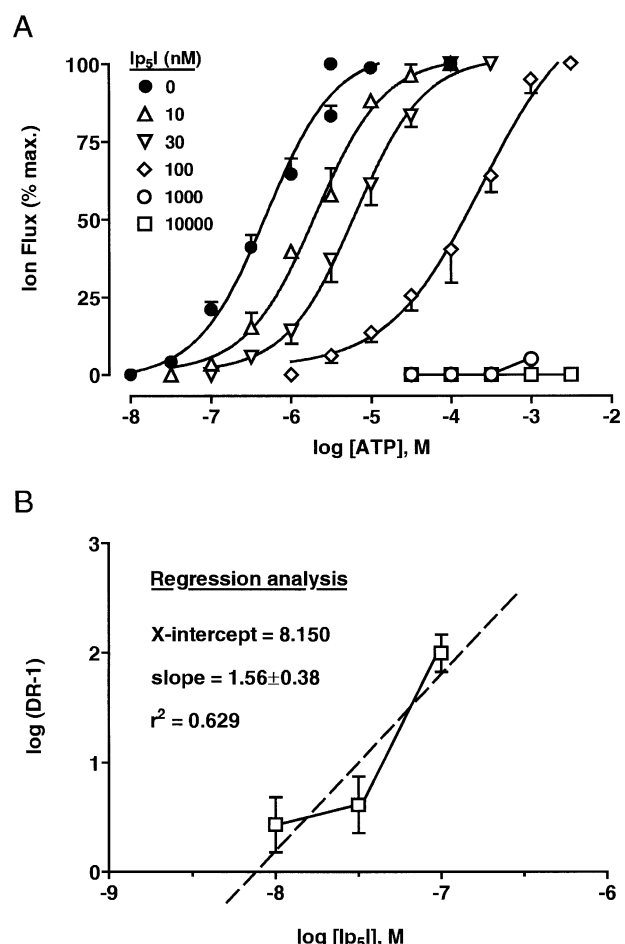


Figure 8 Schild analysis of Ip₅I blockade of rP2X₁ receptors. (A) Concentration/response (C/R) curves for the ATP-activated rP2X₁ receptor, in the absence and presence of Ip₅I (10–10,000 nM). The control C/R curve represented pooled data of 20 determinations, and test C/R curves determined for four experiments for each of the five concentrations of Ip₅I used (10, 30, 100, 1000 and 10,000 nM). (B) The Schild plot of C/R data according to EC₅₀ values stated in Table 2. Linear regression (Prism v2.0, GraphPad) gave an estimated pA₂ of 8.150, mean slope of 1.56 (i.e., greater than unity), and a low correlation coefficient (r^2) of 0.629 for linearity. The Schild plot was clearly biphasic.

ATP effect was reduced by 56 \pm 7% (n=4) by the dinucleotide. Thus, Ip₄I caused a reduction in both agonist potency and efficacy.

At rP2X₃ receptors, Ip₄I (3 μ M, approximate IC₇₅ value) caused a surmountable inhibition of ATP responses (Figure 7B). EC₅₀ values and Hill coefficients for ATP were (for the following Ip₄I concentrations): 0 μ M, 1.0 \pm 0.3 μ M (n_H, 0.82 \pm 0.11); 3 μ M, 17.8 \pm 5.3 μ M (n_H, 0.76 \pm 0.19) (n=4). The pA₂ value for Ip₄I antagonism at rP2X₃ receptors was 6.75 \pm 0.13 (n=4).

Discussion

The present results showed that Ip₅I was an effective antagonist of ATP-responses at Group 1 P2X receptors (P2X₁ and P2X₃), being selective for rP2X₁ receptors at low (\leq 100 nM) concentrations. This pentaphosphate was 900 fold less potent at P2X₃ receptors (comparing IC₅₀ values), at which micromolar concentrations were required to block ATP-activated inward currents. The blocking actions of Ip₅I at P2X₁ receptors at nanomolar concentrations initially seemed

consistent with a competitive antagonism. However, several features suggested that the mechanism of Ip₅I blockade was more complex than originally thought. First, micromolar concentrations of Ip₅I caused a nonsurmountable inhibition of ATP-responses (Figure 8A). Second, determinations of the pA₂ value were dependent on the Ip₅I concentration used (see Table 2). Third, a Schild plot of combined Ip₅I data (10, 30 and 100 nM) was non-linear and the slope (by regression analysis) was greater than unity (Figure 8B). Taken together, these features suggested that Ip₅I is not a simple competitive antagonist at rP2X₁ receptors. Also, the parent compound Ap₅A is a partial agonist at rP2X₁ receptors (Wildman *et al.*, 1999a), suggesting that the binding site for the pentaphosphate (as either Ap₅A or Ip₅I) might not be the same position as the ATP docking site.

For P2X₁ receptors, the blocking activity of the Ip_nI series decreased as the phosphate chain was reduced in length. Thus, Ip₅I was 180 fold more potent than Ip₄I and greater than 10,000 fold more potent than Ip₃I. This potency order for antagonism clearly contrasted with the agonist potency order of their parent compounds at rP2X₁ receptors, where Ap₄A (7.4) > Ap₅A (6.0) > Ap₃A (>4) (pEC₅₀ values) (Wildman *et al.*, 1999a). Like Ip₅I, Ip₄I was a non-competitive antagonist at rP2X₁ receptors and significantly reduced the maximum ATP effect. Its parent compound, Ap₄A, is a partial agonist at rP2X₁ receptors, suggesting the binding site for the tetraphosphate (as either Ap₄A or Ip₄I) might again differ from the ATP docking site. Interestingly, neither dinucleotide triphosphate (Ip₃I and Ap₃A) interacted well with rP2X₁ receptors in terms of antagonist and agonist activities, yet rP2X₁ receptor is activated by a number of mononucleoside triphosphates.

The rP2X₃ receptor showed a slight preference for Ip₄I over Ip₅I, their pA₂ values being 6.75 and 6.27, respectively. Both diinosine compounds appeared to act as competitive antagonists, causing a parallel rightwards shift of the ATP C/R curve without reducing the maximum ATP effect (Figures 6B and 7B). Their parent compounds, Ap₄A and Ap₅A, are both full agonists at rP2X₃ receptors, at which the tetraphosphate (pEC₅₀, 6.10) is slightly more potent than the pentaphosphate (pEC₅₀, 5.88) (Wildman *et al.*, 1999a). As far as the triphosphate is concerned, Ip₃I is a weak antagonist and Ap₃A a partial agonist at rP2X₃ receptors.

The Ip_nI series lacked activity at rP2X₂ receptors at which the parent Ap_nA compounds otherwise showed interesting effects. Ap₄A is a full agonist at rP2X₂ receptors, although 4 fold less potent than ATP, while nanomolar Ap₅A is a potent potentiator of ATP-responses (Pintor *et al.*, 1996). Thus, the inability of Ip₄I and Ip₅I to interact with rP2X₂ receptors contrasted sharply with our earlier results with their parent compounds (Ap₄A and Ap₅A), although the lack of activity of the diinosine polyphosphates at least reflects the efficiency of the enzyme degradation process to make Ip_nI compounds. Ip₅I was reported to be inactive against ATP-responses at P2X₂-like receptors in neonatal rat cerebellar Purkinje neurons, although

Ip₃I and Ip₄I have not yet been tested in this model (Garcia-Lecea *et al.*, 1999).

For rP2X₄ receptors, the potentiating effects of Ip₅I and Ip₄I struck a chord with similar potentiating effects of other compounds (e.g. suramin, PPADS and Reactive blue 2) tested as P2 receptor antagonists at the rat P2X₄ receptor (Bo *et al.*, 1995) and mouse P2X₄ receptor (Townsend-Nicholson *et al.*, 1999). The Ip_nI compounds proved just as ineffective as antagonists at rP2X₄ receptors as other compounds tested so far. The parent dinucleotide of Ip₄I is a partial agonist at rP2X₄ receptors (pEC₅₀, 5.5) (Wildman *et al.*, 1999a). However, the potentiating effect of Ip₄I was not accompanied by any change in holding currents and was not believed to be due to Ap₄A contamination.

Of the Ip_nI series, only Ip₅I has been tested at native P2X receptors. Ip₅I is considerably less potent as an antagonist at the P2X₁-like receptor in guinea-pig vas deferens (pA₂, 6.5 ± 0.1) (Hoyle *et al.*, 1997), compared to its blocking activity at the recombinant rP2X₁ receptor in the present study (pA₂ range, 7.70–9.23). This reduction in activity may be due to Ip₅I breakdown by ecto-nucleotidases in guinea-pig vas deferens, or perhaps due to a difference between guinea-pig and rat P2X₁ receptors. The guinea-pig P2X₁ receptor has not yet been cloned and, furthermore, Ip₅I has not yet been tested on the human P2X₁ receptor. Thus far, the blocking activity of Ip₅I has only been characterized at the rat P2X₁ receptor. Potential species differences in blocking activity notwithstanding, the observed Ip₅I activity at native P2X₁ receptors in guinea-pig still compares favourably with the non-competitive blocking activity of suramin (pK_b, 5.3 ± 0.2), iso-PPADS (pK_b, 6.6 ± 0.2) and Reactive blue 2 (pK_b, 5.8 ± 0.2) at P2X₁-like receptors in rat vas deferens (Khakh *et al.*, 1994). To this end, Ip₅I may yet prove to be a useful pharmacological tool in bioassays of naturally-occurring P2X₁ receptors, for example human HL60 cells (Buell *et al.*, 1996) and murine thymocytes (Chavtcho *et al.*, 1996) as well as P2X₁-like receptors in vas deferens and vascular smooth muscle of various mammalian species (Humphrey *et al.*, 1998).

References

BO, X., ZHANG, Y., NASSAR, M., BURNSTOCK, G. & SCHOEPFER, R. (1995). A P2X purinoreceptor cDNA conferring a novel pharmacological profile. *FEBS Lett.*, **375**, 129–133.

BUELL, G., MICHEL, A.D., LEWIS, C., COLLO, G., HUMPHREY, P.P. & SURPRENANT, A. (1996). P2X₁ receptor activation in HL60 cells. *Blood*, **87**, 2659–2664.

CHAVTCHO, Y., VALERA, S., AUBRY, J.P., RENNO, T., BUELL, G. & BONNEFOY, J.Y. (1996). The involvement of an ATP-gated ion channel, P(2X1), in thymocyte apoptosis. *Immunity*, **5**, 275–283.

COLLO, G., NORTH, R.A., KAWASHIMA, E., MERLO-PICH, E., NEIDHART, S., SURPRENANT, A. & BUELL, G. (1996). Cloning of P2X₅ and P2X₆ receptors and the distribution and properties of an extended family of ATP-gated ion channels. *J. Neurosci.*, **16**, 2495–2507.

EVANS, R.J., LEWIS, C., BUELL, G., VALERA, S., NORTH, R.A. & SURPRENANT, A. (1995). Pharmacological characterization of heterologously expressed ATP-gated cation channels (P₂X purinoreceptors). *Mol. Pharmacol.*, **48**, 178–183.

EVANS, R.J. & SURPRENANT, A. (1996). P2X receptors in autonomic and sensory neurons. *Semin. Neurosci.*, **8**, 217–223.

EVANS, R.J., SURPRENANT, A. & NORTH, R.A. (1998). P2X receptors: Cloned and Expressed. In: Turner J.T., Weisman G.A. & Fedan J.S. (eds). *The P2 Nucleotide Receptors*. Humana Press, New Jersey, Ch. 2, pp 43–62.

GARCIA-LECEA, M., DELICADO, E.G., MIRAS-PORTUGAL, M.T. & CASTRO, E. (1999). P2X₂ characteristics of the ATP receptor coupled to $[Ca^{2+}]_i$ increases in cultured Purkinje neurons from neonatal rat cerebellum. *Neuropharmacol.*, **38**, 699–706.

GURANOWSKI, A.E., STARZYNSKA, E., GÜNTHER SILLERO, M.A. & SILLERO, A. (1995). Conversion of adenosine(5')oligophospho(5')adenosines into inosine(5')oligophospho(5')inosines by non-specific adenylate deaminase from the snail *Helix pomatia*. *Biochim. Biophys. Acta*, **1243**, 78–84.

HOYLE, C.H.V., PINTOR, J., GUALIX, J. & MIRAS-PORTUGAL, M.T. (1997). Antagonism of P2X receptors in guinea-pig vas deferens by diinosine pentaphosphate. *Eur. J. Pharmacol.*, **333**, R1–R2.

HUMPHREY, P.P.A., KHAKH, B.S., KENNEDY, C., KING, B.F. & BURNSTOCK, G. (1998). Nucleotide receptors: P2X receptors. In: *IUPHAR Compendium of Receptor Characterization and Classification*. IUPHAR Media Publications, pp 195–208.

HUMPHREYS, B.D., VIRGINIO, C., SURPRENANT, A., RICE, J. & DUBYAK, G.R. (1998). Isoquinolines as antagonists of the P2X₇ nucleotide receptor: high selectivity for the human versus rat receptor homologues. *Mol. Pharmacol.*, **54**, 22–32.

JACOBSON, K.A., KIM, Y.C., WILDMAN, S.S., MOHANRAM, A., HARDEN, K., BOYER, J.L., KING, B.F. & BURNSTOCK, G. (1998). A pyridoxine cyclic phosphate and its 6-azoaryl-derivative selectively potentiate and antagonize activation of P2X₁ receptors. *J. Med. Chem.*, **41**, 2201–2206.

KHAKH, B.S., MICHEL, A. & HUMPHREY, P.P.A. (1994). Estimates of antagonist affinities at P_{2X} purinoceptors in rat vas deferens. *Eur. J. Pharmacol.*, **263**, 301–309.

KIM, M., YOO, O.J. & CHOE, S. (1997). Molecular assembly of the extracellular domain of P2X₂, an ATP-gated ion channel. *Biochem. Biophys. Res. Comm.*, **240**, 618–622.

KING, B.F. (1998). Molecular Biology of P2X Purinoceptors. In: Burnstock G., Dobson J.G., Liang B.T. & Linden J. (eds). *Cardiovascular Biology of Purines*. Kluwer Academic Publications, Massachusetts, Ch. 10, pp 159–186.

KING, B.F., ZIGANSHINA, L.E., PINTOR, J. & BURNSTOCK, G. (1996). Full sensitivity of P2X₂ purinoceptor to ATP revealed by changing extracellular pH. *Br. J. Pharmacol.*, **117**, 1371–1373.

KUPITZ, Y. & ATLAS, D. (1993). A putative ATP-activated Na^+ channel involved in sperm-induced fertilization. *Science*, **261**, 484–486.

NICKE, A., BÄUMERT, H.G., RETTINGER, J., EICHELE, A., LAM-BRECHT, G., MUTSCHLER, E. & SCHMALZING, G. (1998). P2X₁ and P2X₃ receptors form stable trimers: a novel structural motif of ligand-gated ion channels. *EMBO J.*, **17**, 3016–3028.

PINTOR, J., DÍAZ-HERNÁNDEZ, M., BUSTAMANTE, C., GUALIX, J., DE TERREROS, F.J. & MIRAS-PORTUGAL, M.T. (1999). Presence of dinucleotide and ATP receptors in human cerebrocortical synaptic terminals. *Eur. J. Pharmacol.*, **366**, 159–165.

PINTOR, J., GUALIX, J. & MIRAS-PORTUGAL, M.T. (1997). Diinosine polyphosphates, a group of dinucleotides with antagonistic effects on diadenosine polyphosphate receptor. *Mol. Pharmacol.*, **51**, 277–284.

PINTOR, J., KING, B.F., MIRAS-PORTUGAL, M.T. & BURNSTOCK, G. (1996). Selectivity and activity of adenine dinucleotides at recombinant P2X₂ and P2Y₁ receptors. *Br. J. Pharmacol.*, **119**, 1006–1012.

RAE, M.G., ROWAN, E.G. & KENNEDY, C. (1998). Pharmacological properties of P2X₃-receptors present in neurones of the rat dorsal root ganglia. *Br. J. Pharmacol.*, **124**, 176–180.

RALEVIC, V. & BURNSTOCK, G. (1998). Receptors for purines and pyrimidines. *Pharmacol. Rev.*, **50**, 413–492.

SOTO, F., LAMBRECHT, G., NICKE, P., STUHMER, W. & BUSCH, A.E. (1999). Antagonistic properties of the suramin analogue NF023 at heterologously expressed P2X receptors. *Neuropharmacol.*, **38**, 141–149.

TORRES, G.E., EGAN, T.M. & VOIGT, M.M. (1999). Hetero-oligomeric assembly of P2X receptor subunits. *J. Biol. Chem.*, **274**, 6653–6659.

TOWNSEND-NICHOLSON, A., KING, B.F., WILDMAN, S.S. & BURNSTOCK, G. (1999). Molecular cloning, functional characterization and possible cooperativity between the murine P2X₄ and P2X_{4a} receptors. *Mol. Brain. Res.*, **64**, 246–254.

VIRGINIO, C., ROBERTSON, G., SURPRENANT, A. & NORTH, R.A. (1998). Trinitrophenyl-substituted nucleotides are potent antagonists selective for P2X₁, P2X₃, and heteromeric P2X receptors. *Mol. Pharmacol.*, **53**, 969–973.

WILDMAN, S.S., BROWN, S.G., KING, B.F. & BURNSTOCK, G. (1999a). Selectivity of diadenosine polyphosphates for rat P2X receptor subunits. *Eur. J. Pharmacol.*, **367**, 119–123.

WILDMAN, S.S., KING, B.F. & BURNSTOCK, G. (1999b). Modulation of ATP-responses at recombinant rP2X₄ receptors by extracellular pH and Zinc. *Br. J. Pharmacol.*, **126**, 762–768.

WILDMAN, S.S., KING, B.F. & BURNSTOCK, G. (1999c). Modulatory activity of extracellular H^+ and Zn^{2+} on ATP-responses at rP2X₁ and rP2X₃ receptors. *Br. J. Pharmacol.*, **128**, 486–492.

(Received June 3, 1999)

Revised July 29, 1999

Accepted August 11, 1999